A compact broadband microfiber Bragg grating

Ming Ding,* Michalis N. Zervas, and Gilberto Brambilla

Optoelectronics Research Centre, University of Southampton, Southampton, SO17 1BJ, UK
**md20g09@orc.soton.ac.uk*

Abstract: A sub-10μm long microfiber Bragg grating was nanostructured into a ~1μm-diameter optical microfiber by focused ion beam (FIB) technology. The periodic structures were carved into the microfiber and the large refractive index contrast between glass and air allowed for the formation of strong gratings with only 20 periods. 3D simulation showed a good agreement with the experiment demonstration. This compact device can find applications in a variety of fields ranging from temperature and refractive index sensing to optical communications.

OCIS codes: (230.1150) All-optical devices; (060.3735) Fiber Bragg gratings; (060.4005) Microstructured fibers; (220.4241) Nanostructure fabrication.

References and links

1. K. O. Hill, Y. Fujii, D. C. Johnson, and B. S. Kawasaki, "Photosensitivity in optical fiber waveguides: application to reflection filter fabrication," Appl. Phys. Lett. **32**(10), 647–649 (1978).
2. B. S. Kawasaki, K. O. Hill, D. C. Johnson, and Y. Fujii, "Narrow-band Bragg reflectors in optical fibers," Opt. Lett. **3**(2), 66–68 (1978).
3. R. Kashyap, *Fiber Bragg Grating* (Elsevier Academic, 2010).
4. G. Meltz, W. W. Morey, and W. H. Glenn, "Formation of Bragg gratings in optical fibers by a transverse holographic method," Opt. Lett. **14**(15), 823–825 (1989).
5. K. O. Hill, B. Malo, F. Bilodeau, D. C. Johnson, and J. Albert, "Bragg grating fabricated inmonomode photosensitive optical fiber by UV exposure through a phase mask," Appl. Phys. Lett. **62**(10), 1035–1037 (1993).
6. G. Pakulski, R. Moore, C. Maritan, F. Shepherd, M. Fallahi, I. Templeton, and G. Champion, "Fused silica masks for printing uniform and phase adjusted gratings for distributed feedback lasers," Appl. Phys. Lett. **62**(3), 222–224 (1993).
7. M. J. Cole, W. H. Loh, R. I. Laming, M. N. Zervas, and S. Barcelos, "Moving fiber/phase mask-scanning beam technique for enhanced flexibility in producing fiber gratings with uniform phase mask," Electron. Lett. **31**(17), 1488–1490 (1995).
8. D. C. Johnson, F. Bilodeau, B. Malo, K. O. Hill, P. G. J. Wigley, and G. I. Stegeman, "Long-length, long-period rocking filters fabricated from conventional monomode telecommunications optical fiber," Opt. Lett. **17**(22), 1635–1637 (1992).
9. C. W. Smelser, S. J. Mihailov, and D. Grobnic, "Hydrogen loading for fiber grating writing with a femtosecond laser and a phase mask," Opt. Lett. **29**(18), 2127–2129 (2004).
10. A. Dragomir, D. N. Nikogosyan, K. A. Zagorulko, P. G. Kryukov, and E. M. Dianov, "Inscription of fiber Bragg gratings by ultraviolet femtosecond radiation," Opt. Lett. **28**(22), 2171–2173 (2003).
11. H. Xuan, W. Jin, and S. Liu, "Long-period gratings in wavelength-scale microfibers," Opt. Lett. **35**(1), 85–87 (2010).
12. J. D. Love, W. M. Henry, W. J. Stewart, R. J. Black, S. Lacroix, and F. Gonthier, "Tapered single-mode fibers and devices. I. Adiabaticity criteria," IEE Proc.-J.:Optoelectron. **138**, 343–354 (1991).
13. F. Bilodeau, K. O. Hill, S. Faucher, and D. C. Johnson, "Low-loss highly overcoupled fused couplers: fabrication and sensitivity to external pressure," J. Lightwave Technol. **6**(10), 1476–1482 (1988).
14. G. Brambilla, E. Koizumi, X. Feng, and D. J. Richardson, "Compound-glass optical nanowires," Electron. Lett. **41**(7), 400–401 (2005).
15. T. A. Birks and Y. W. Li, "The shape of fiber tapers," J. Lightwave Technol. **10**(4), 432–438 (1992).
16. G. Brambilla, V. Finazzi, and D. J. Richardson, "Ultra-low-loss optical fiber nanotapers," Opt. Express **12**(10), 2258–2263 (2004).
17. Y. Jung, G. Brambilla, and D. J. Richardson, "Optical microfiber coupler for broadband single-mode operation," Opt. Express **17**(7), 5273–5278 (2009).
18. R. Feced and M. N. Zervas, "Effects of random phase and amplitude errors in optical fiber Bragg gratings," J. Lightwave Technol. **18**(1), 90–101 (2000).

1. Introduction

Optical fiber Bragg grating (FBG) has played an important role in optical communication and optical sensors in the last decades. By a periodic variation to the refractive index of the fiber

#149337 - $15.00 USD Received 15 Jun 2011; revised 15 Jul 2011; accepted 15 Jul 2011; published 29 Jul 2011

core, the reflected signal centered at Bragg wavelength is observed. The first permanent FBG was demonstrated by K. O. Hill *et al.* in 1978 using an argon ion laser radiation [1,2]. After that, several technologies were used to inscribe FBGs [3], e.g. bulk interference [4], phase mask interference [5–7] and point by point writing [8]. Laser induced gratings rely on the fiber photosensitivity to induce a very small refractive index modulations (typically $\Delta n \sim 10^{-4}$-10^{-3}). The inscription of relatively long uniform Bragg gratings with small Δn resulted in a bandwidth of the order of 1nm. In recent years femtosecond (*fs*) lasers [9,10] have been used to write gratings in range of materials which include also pure silica and ZBLAN glasses, previously considered insufficiently photosensitive for other lasers. Indeed, *fs* lasers have also been used to ablate the surface of microfibers [11] and exploit the periodic surface damage to write long period gratings; the large refractive index contrast (Δn ~0.45) between silica and air resulted in a long period grating length of ~150μm. In this paper, we demonstrate the possibility to inscribe a microfiber Bragg grating (MFBG) by nanostructuring a microfiber with focused ion beam (FIB) milling. FIB milling allows for an extreme flexibility in the grating design, as it is a direct writing technique. The size and the shape of individual grating elements can be controlled over a wide range of values in a straightforward manner. In addition to Bragg wavelength this results in control of the out-of-plane scattering and radiation losses. Twenty specially shaped notches were carved in the microfiber and thus achieved a $\Delta n \sim 0.446$ at the wavelength $\lambda = 1.4\mu m$ allowing for a grating length smaller than 10μm which is the shortest FBG to our knowledge.

2. Microfiber Bragg grating

2.1. Working principle and fabrication

Figure 1 represents a schematic of MFBG, which is composed of dozens of groves inscribed in the uniform waist region of a microfiber connected by two conical transition regions to conventional optical fibers. When the tapered transition region is adiabatic, the fundamental mode of the fiber shows no power exchange with the high order mode and can be guided continuously from core mode to cladding mode [12]. The diameter of the uniform waist region was chosen to be d~1μm, thus the microfiber operated in single mode regime above λ~1μm.

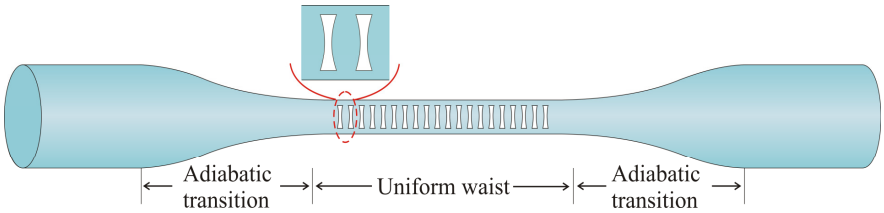

Fig. 1. Schematic of MFBG. The insert shows a schematic of the biconcave shape of curved air notches.

When a microfiber is periodically machined, air cavities are formed; by exploiting the refractive index difference between silica and air, Δn as high as ~0.446 at $\lambda = 1.4\mu m$ can be achieved. At each silica/air interface a fraction of the propagating light is reflected and the repeated refractive index modulations result in multiple reflections of the forward and backscattered travelling lights which interfere to give transmission and reflection spectra. The refractive index modulation periodicity and the light wavelength determine the relative phase with which all reflected signals are combined together. At a particular wavelength, known as the Bragg wavelength, all reflected signals are in phase and add constructively and a back reflected signal centered at the Bragg wavelength is observed. Reflected contributions from light at other wavelength do not add constructively and are cancelled out; as a result these wavelengths are transmitted through the grating. Due to the high refractive index contrast between silica and air, reflection is strong at each interface, meaning that only ~70 periods are needed to obtain 99% reflectivity in standard telecom fibers. Inevitably, such large refractive

#149337 - $15.00 USD Received 15 Jun 2011; revised 15 Jul 2011; accepted 15 Jul 2011; published 29 Jul 2011

index changes result in relatively strong radiation-mode excitation and losses. In order to decrease the radiation loss, the air cavities were designed with a biconcave geometry (shown schematically in Fig. 1). This effectively results in a periodic series of small biconvex lens-like structures that better confine the light and reduce radiation losses. If a fiber with high refractive index core is used, the refractive index contrast between fiber and air is larger and the grating period number can be decreased even further.

In this study, a standard telecom optical fiber (Corning SMF-28) was used to fabricate the microfiber. The low loss microfiber was manufactured by the well-established microheater brushing technique [13,14]. The profile of the conical transition tapers in the experiment was approximated by a decreasing exponential function (transition region length ~25mm, uniform waist length ~4mm, relative taper elongation rate = 0 [15]) and was achieved by ensuring appropriate control of the translation stage movement during the tapering process [15,16]. The microfiber diameter was d~1.34μm and allowed single mode propagation at λ>~1μm and multimode operation at shorter wavelengths. The microfiber was packaged on an aluminum slide which was coated by a layer of Efiron PC-373 (Luvantix, Ansan-si, Korea), having a cured refractive index of n~1.373@1550nm, to avoid additional optical losses. To increase device sturdiness, part of the microfiber was embedded in the low refractive index polymer and the microfiber pigtails were fixed to the slide using two small drops of UV curable polymer (UV375, still from Luvantix). A 100nm layer of gold was deposited on the taper surface by an electron beam evaporator to avoid charging during FIB milling which can cause large fabrication errors. The grating period was chosen to be Λ~506nm to obtain the first order

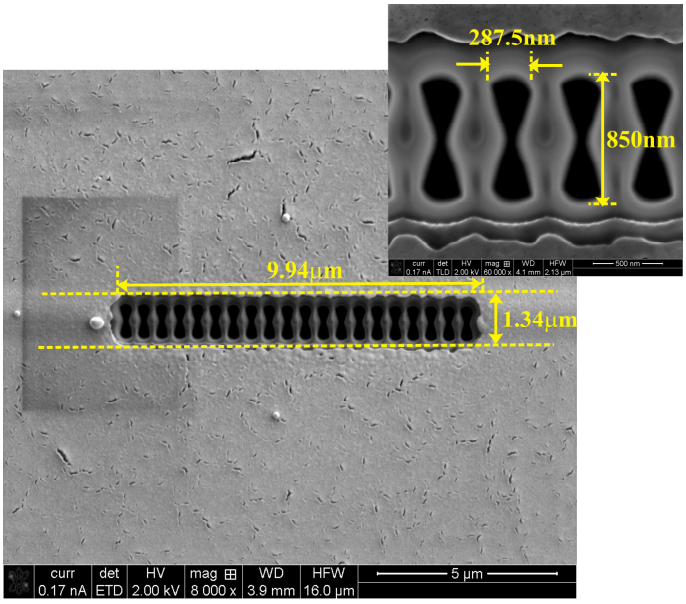

Fig. 2. SEM image of MFBG which was partly embedded in the polymer and coated with a gold layer. Yellow dashed lines visualize the microfiber edge, which is not clear because the microfiber was packaged in polymer and gold coated. The insert shows the details of the biconcave air notches.

Bragg reflection at λ_B~1360nm. In order to optimize the length ratio of the air and silica, we did simply calculation by using an infinite periodically multilayer which has the same refractive index with the MFBG. The reflectivity has maximum when the notch length is 210nm~310nm. The FEI "Helios 600" FIB system was used to etch the cavities with gallium ion beam characterized by a 30.0kV accelerating voltage and 93pA current. Biconcave air cavities 287.5nm long × 850nm wide were centrally and precisely curved-out along the waist

#149337 - $15.00 USD Received 15 Jun 2011; revised 15 Jul 2011; accepted 15 Jul 2011; published 29 Jul 2011

of the microtapered fiber. Features with less than 20nm width can be easily achieved with this specific ion beam.

Figure 2 shows the SEM image of the gold-coated MFBG with 20 periods. The total length of the MFBG is 9.4μm, which is extremely short compared with conventional FBGs (a few millimeters or centimeters). Gold was consequently removed using gold etchant after FIB milling.

2.2. Optical reflection properties

The MFBG reflection properties were characterized using the set-up showed in Fig. 3(a). A supercontinuum (SC) source (Fianium Ltd, Southampton, U. K.) was used to deliver light over a rather broad range of wavelengths (450nm-1800nm) with maximum pulse energy of 50nJ. The fiberized laser output was angle-cleaved to avoid back reflections from the optical components. Light from the SC source was launched into a bi-conical 2 × 2 microfiber coupler with an extremely wide single mode operation bandwidth (400nm-1700nm) [17]. This coupler is specifically designed to suppress any higher order mode content present at the input fiber whilst at the same time providing efficient power splitting into the fundamental mode equally at the two output ports. One of the output ports was connected with the MFBG. Light reflected by the grating passed through the coupler and was recorded by an optical spectrum analyser (AQ6317, Yokogawa, Japan). XYZ stages were used to align the different fiber components.

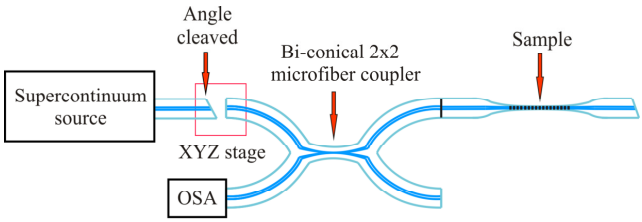

(a)

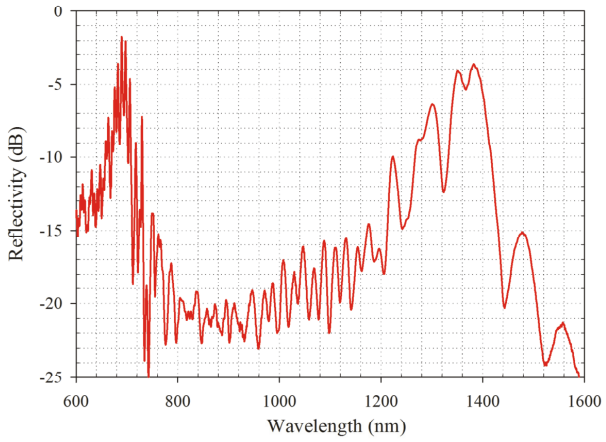

(b)

Fig. 3. (a) Schematic of experimental set-up used to characterize the MFBG; (b) MFBG reflection spectrum.

The spectral response of the coupler output was firstly recorded without any sample to provide a normalization base line for the following spectra and to remove any wavelength dependence related to the source and to the coupler. Then, the sample reflection spectra were recorded.

Figure 3(b) shows the MFBG reflection spectrum. There are two peaks in this spectrum. The peak at λ~1360nm corresponds to the first order Bragg reflection for the fundamental

#149337 - $15.00 USD Received 15 Jun 2011; revised 15 Jul 2011; accepted 15 Jul 2011; published 29 Jul 2011

mode, while that one at λ~680nm comes from the second order Bragg reflection. The width of the fundamental mode peak is ~75nm, considerably broader than that observed in uniform FBGs (~1nm) written in conventional fibers. Strong reflection (−3dB corresponds to 50% reflection) was observed with only 20 periods MFBG. The reflectivity response (amplitude and width of the Bragg peak) can be further optimized by optimizing a number of physical parameters for the MFBG, such as the grating period number, their shape and the microfiber material.

3. Modeling of microfiber grating

To verify the experimental results, 3D Finite Element Method (FEM) were used to numerically solve Maxwell equations in the frequency domain and get the electric field and reflectivity of the MFBG. The numerical model was defined, solved and analyzed using COMSOL 4.1 multiphysics. The modeling geometry is presented in Fig. 4 (a) and it has the same geometry with the MFBG shown in the SEM image of Fig. 2. The highlight lines in Fig. 4 (a) insert shows the biconcave air notch profile. The MFBG is surrounded by polymer which has refractive index n~1.373. In order to decrease calculation complexity and time, symmetry was used to reduce the geometry to a half of cylinder. The chosen boundary conditions were: perfect electric conductor (flat surface at the top in Fig. 4(a)) at the symmetry planes, scattering boundary condition at the cylinder outer surfaces and port boundary at the input and output surfaces. Simulations were run with controlled mesh size (150nm in silica, 250nm in polymer and 75nm in air notches) to make efficient use of computer memory. A single mode was launched into the MFBG from the input port. Figure 4(b), 4(c) and 4(d) which corresponds the wavelengths λ_1, λ_2 and λ_3 in Fig. 5 show the electric field of the grating at the Bragg wavelength and at wavelengths far from the Bragg condition. The field distribution in Fig. 4(c) confirms that the reflection peak around the 1364nm indeed corresponds to the main Bragg wavelength; on the contrary, far from the Bragg wavelength, at the minimum reflection points as shown in Fig. 4(b) and 4(d), almost all the light passes through the grating.

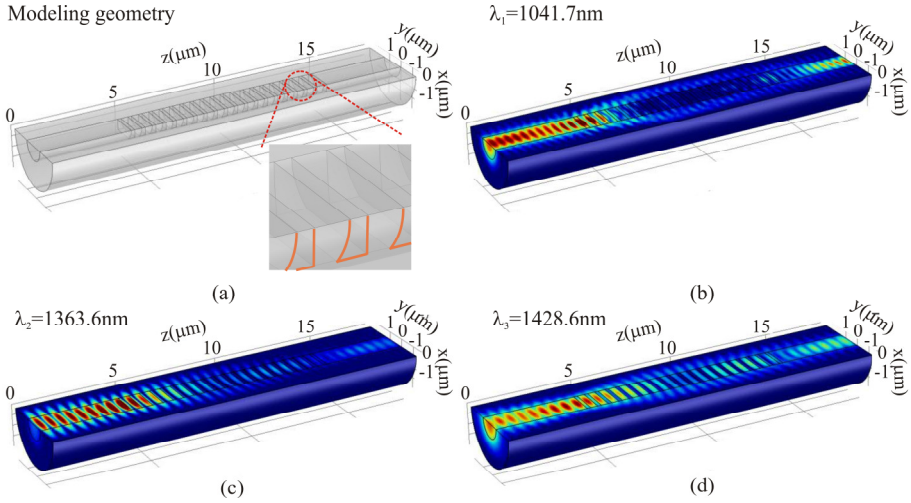

Fig. 4. (a) Schematic of the MFBG modeling, the insert shows the magnified figure of the biconcave air notch; (b)(c)(d) Electric fields at wavelength λ_1 = 1041.7nm, λ_2 = 1363.6nm and λ_3 = 1428.6nm respectively.

Figure 5 presents the theoretical reflectivity against the wavelength (the red solid line) which was evaluated using the S-parameter function in COMSOL 4.1 multiphysics. As for the experiment (reported in dashed blue for reference), numerical calculation shows a reflection peak at λ~1364nm. The two graphs show few differences, like a different periodicity, a double Bragg peak in reflection and wavelength shift. A possible explanation might be related to the different polarization conditions: while in the experiment light was not polarized, simulations

#149337 - $15.00 USD Received 15 Jun 2011; revised 15 Jul 2011; accepted 15 Jul 2011; published 29 Jul 2011

allowed for only one linear polarization. Moreover, since the upper part of the MFBG is surrounded by air in the experiment, the two polarizations experience different surroundings, thus a different effective refractive index. Possible explanations for the other spectral mismatches include the presence of unwanted high order modes in the polymer cladding, the only-partial grating embedding in the experiments, or different effective indices of the mode propagating in the microfiber between experiments and simulations due to diameter fluctuation and/or residual stresses. Finally, small imperfections in periodicity and/or lateral position the grating notches can amount to small spatial phase and grating strength error, which were known to affect the grating reflectivity more severely in the out-of-band spectral region [18].

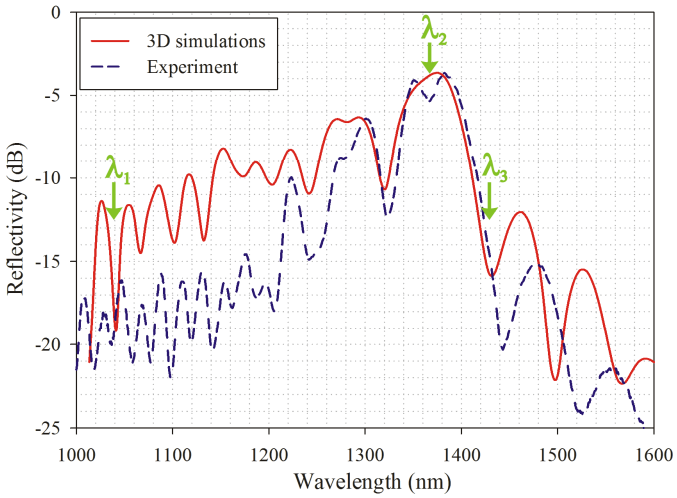

Fig. 5. MFBG reflectivity spectra. The red solid line is the 3D simulation line while the blue dashed line is the experiment result. λ_1, λ_2 and λ_3 represent the wavelengths whose electric fields are shown in Fig. 4(b), 4(c) and 4(d).

4. Conclusions

In conclusion, a robust and extremely short MFBG has been manufactured by inscribing periodic biconcave air notches in a microfiber using FIB milling. A strong reflection peak was observed in the experiments. 3D COMSOL simulations were carried out to verify the experiment result. This compact MFBG can find a wealth of applications and be widely used in sensing. In the sensor application field, the size of grating is a key issue. While the size of the conventional FBG is limited by Δn and fiber diameter, in a microfiber with only few microns diameter, the grating size can be decreased drastically and the presence of a strong evanescent field can increase the sensor sensitivity to environment properties.

Acknowledgments

G. Brambilla gratefully acknowledges the Royal Society (UK) for his University Research Fellowship.

#149337 - $15.00 USD Received 15 Jun 2011; revised 15 Jul 2011; accepted 15 Jul 2011; published 29 Jul 2011